AIP | Applied Physics Letters

High transmission acoustic focusing by impedance-matched acoustic meta-surfaces

Rasha Al Jahdali and Ying Wu

Citation: Applied Physics Letters **108**, 031902 (2016); doi: 10.1063/1.4939932
View online: http://dx.doi.org/10.1063/1.4939932
View Table of Contents: http://scitation.aip.org/content/aip/journal/apl/108/3?ver=pdfcov
Published by the AIP Publishing

High transmission acoustic focusing by impedance-matched acoustic meta-surfaces

Rasha Al Jahdali and Ying Wu[a)]
Division of Mathematical and Computer Sciences and Engineering, King Abdullah University of Science and Technology (KAUST), Thuwal 23955-6900, Saudi Arabia

(Received 24 November 2015; accepted 3 January 2016; published online 19 January 2016)

Impedance is an important issue in the design of acoustic lenses because mismatched impedance is detrimental to real focusing applications. Here, we report two designs of acoustic lenses that focus acoustic waves in water and air, respectively. They are tailored by acoustic meta-surfaces, which are rigid thin plates decorated with periodically distributed sub-wavelength slits. Their respective building blocks are constructed from the coiling-up spaces in water and the layered structures in air. Analytic analysis based on coupled-mode theory and transfer matrix reveals that the impedances of the lenses are matched to those of the background media. With these impedance-matched acoustic lenses, we demonstrate the acoustic focusing effect by finite-element simulations. © *2016 AIP Publishing LLC*. [http://dx.doi.org/10.1063/1.4939932]

Acoustic lenses can focus or manipulate acoustic waves. They have attracted interest due to their broad applications in various domains, such as biomedical imaging and surgery.[1–3] Acoustic lenses have been devised to achieve various functionalities. For example, phononic crystal-based acoustic lenses have been designed[4] and fabricated[5] to focus incident acoustic waves. Space-coiling structures have been utilized in the design of gradient acoustic lenses.[6–10] With gradient acoustic lenses, acoustic radiation patterns, such as focusing,[6,8–11] tunable transmission,[7,12,13] reflection,[10] and cylindrical-to-plane wave conversion,[9] can be manipulated. Very recently, acoustic meta-surfaces have been used in the design of acoustic lenses. Acoustic meta-surfaces are planarized metamaterials that consist of carefully designed sub-wavelength building blocks. They have exceptional functionality in controlling acoustic waves, including perfect absorption,[14] collimation,[15,16] extraordinary transmission,[17] reflection,[18] wavefront steering,[19] unidirectional transmission,[20] and negative refraction.[21]

In the study of acoustic lenses, especially in the transmitted domain, impedance is an important issue because mismatched impedance of an acoustic lens to the environment is detrimental to the performance of the acoustic lens. Much effort has been devoted to reducing the impact of mismatched impedance.[6,8,9,11,15,20,22–29] One way to do so is to utilize Fabry-Perot (FP) resonances,[6,8,15,20,22,29] which can increase the transmission energy because of the destructive interference between the multiple reflections of acoustic waves on the input and output surfaces of the acoustic lens. Because the resonant frequency of FP resonances is sensitive to the effective thickness of the acoustic lens, it may not be able to perfectly eliminate the reflection in real applications. The performance of the acoustic lens is still affected by the mismatched impedance.

Here, we propose two types of impedance-matched acoustic lenses to focus acoustic waves in water and air, respectively. They are tailored by acoustic meta-surfaces. The building blocks of the acoustic lens in water are constructed from coiling-up spaces.[21] The coupled-mode theory is used to deduce the effective medium parameters of the lens. By choosing the proper material to fill up the coiling-up spaces, we match the effective impedance of the lens to that of the background. We utilize layered media as the building blocks of the acoustic lens in air. By optimizing the thickness and sequence of the layers of different materials, we match the input impedance of the acoustic lens to the impedance of air so that the reflection is minimized. We demonstrate the focusing effect of both types of lenses by finite-element simulations, which show that high energy is transmitted through the lenses over a broad frequency range because of matched impedance and the intrinsic non-resonance-based mechanism. These designable lenses are experimentally feasible and may be beneficial to real wave-energy applications.

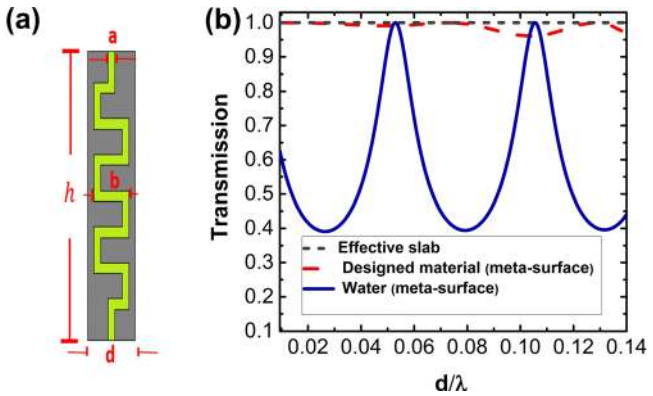

FIG. 1. (a) Schematic of the building block of the meta-surface. The gray area indicates the rigid slab. (b) The transmission spectrum of a plane wave incident on the meta-surface with the periodically distributed structure illustrated in Fig. 1(a). The red dashed curve and the blue solid curve correspond to the cases where slits are filled with the designed material and water, respectively. The black dotted curve corresponds to the transmission spectrum of the same plane wave incident on an effective homogenous slab of the designed metasurface.

[a)]Email: Ying.Wu@kaust.edu.sa

A schematic of the coiling-up spaces used as building blocks for the acoustic lens in water is presented in Fig. 1(a). It is a steel slab perforated with periodic curled slits immersed in water. The geometric parameters h, a, and b represent the thickness of the plate, the width of the slits, and the length of one horizontal segment of the curled slits, respectively. d represents the periodicity of the structure, which is the distance between the adjacent slits. Each slit is filled with a material that has mass density, ρ_s, and wave velocity, c_s, which are determined by $\rho_s = (a/d)\,\rho_0$ and $c_s = c_0$, respectively. ρ_0 and c_0 denote the mass density and wave velocity of water. In the literature, various homogenization schemes have been developed to characterize the effective medium properties of structures associated with coiling-up spaces, such as an S-parameter retrieval method[30] and parameter retrieval method.[8,31] Here, we will analytically explore the effective medium properties of the coiling-up space from coupled-mode theory.[32,33] The transmission and reflection coefficients of the structure shown in Fig. 1(a) are derived as follows. Suppose a plane wave incident from the bottom along the vertical direction. The expression of the pressure field below and above the slab can be, respectively, written as

$$p_I = \sum_{\tau} (\delta_{0,\tau} e^{i\alpha_\tau z} + r_\tau e^{-i\alpha_\tau z}) e^{iG_\tau x} \tag{1}$$

and

$$p_{III} = \sum_{\tau} t_\tau e^{i\alpha_\tau (z-h)} e^{iG_\tau x}, \tag{2}$$

where $\delta_{0,\tau}$ is the Kronecker delta, and $G_\tau = 2\pi\tau/d$ and $\alpha_\tau = \sqrt{k_0^2 - G_\tau^2}$ are the momentum of the τ th diffraction order along the x and z directions, respectively. k_0 $(= \omega/c_0)$ is the wave-vector of the incident wave in water (ω is the angular frequency). r_τ and t_τ denote the normalized pressure field amplitudes of the τ th diffraction order of reflected and transmitted waves, respectively. Inside the slit, the pressure field is expanded in terms of the waveguide modes, because the width of the slit is much smaller than the wavelength and only the zero-order propagation mode is supported. Thus, the pressure field inside the slit is defined as

$$p_{II} = Ae^{ik_s z'} + Be^{-ik_s z'}, \tag{3}$$

where A and B are the corresponding amplitudes of pressure fields of the upward and downward propagating waves, respectively. $k_s = \omega/c_s$ is the wave vector inside the curled slits, and z' indicates the distance from the inlet of the slit to a point inside the slit. At the outlet of the slit, $z' = h_t$, where h_t is the total length of the curled slit. The continuity condition requires that the pressure fields and normal velocity at the interfaces between the slits and the water (i.e., at $z = 0$ (or $z' = 0$) and $z = h$ (or $z' = h_t$)) be continuous. Combining the continuity conditions with Eqs. (1)–(3), we can solve for the coefficients r_τ and t_τ. In the low-frequency or long-wavelength regime ($\lambda > d$), only the zero-order diffracted wave is the propagating mode. All the other higher-order modes are evanescent, because α_τ is imaginary. Thus, the far-field transmission and reflection coefficients can be expressed as

$$t_0 = \frac{4f(\xi_0/\xi_s)e^{ik_s h_t}}{[f(\xi_0/\xi_s)+1]^2 - e^{2ik_s h_t}[f(\xi_0/\xi_s)-1]^2} \tag{4}$$

$$r_0 = \frac{\left[1 - f^2(\xi_0/\xi_s)^2\right] + e^{2ik_s h_t}\left[f^2(\xi_0/\xi_s)^2 - 1\right]}{[f(\xi_0/\xi_s)+1]^2 - e^{2ik_s h_t}[f(\xi_0/\xi_s)-1]^2},$$

where $f = a/d$ is the ratio of the width of the slit to the periodicity. On the other hand, the transmission and reflection amplitudes of a plane wave normally incident on a homogenous slab with thickness h are written, respectively, as

$$\hat{T}(\omega) = \frac{4(\xi_0/\xi_{eff})e^{ik_{eff}h}}{(\xi_0/\xi_{eff}+1)^2 - e^{2ik_{eff}h}(\xi_0/\xi_{eff}-1)^2} \tag{5}$$

$$\hat{R}(\omega) = \frac{\left(1 - (\xi_0/\xi_{eff})^2\right) + e^{2ik_{eff}h}\left((\xi_0/\xi_{eff})^2 - 1\right)}{(\xi_0/\xi_{eff}+1)^2 - e^{2ik_{eff}h}(\xi_0/\xi_{eff}-1)^2}.$$

Comparing Eqs. (4) and (5), we notice a certain correspondence between the meta-surface and the homogenous slab. If we treat the meta-surface as a homogeneous slab, its effective refractive index and effective impedance is given as $n_{eff} = (h_t/h)n_s$ and $\xi_{eff} = (1/f)\xi_s$, respectively. Interestingly, the impedance of the material inside the slits is given by $\xi_s = (a/d)\,\xi_0$, which means that the effective impedance exactly matches the impedance of the water background, ξ_0. Total transmission is therefore expected even though the width of the slit is narrow. In Fig. 1(b), we plot the transmission coefficients of a meta-surface with $a = 0.19d$, $h = 6d$, and $b = 0.65d$ chosen as the geometric parameters and with the slit folded six times (so that the total length of the slit, h_t, is $9.9d$). Since this design does not rely on resonance, nearly total transmission is observed over the frequency range of $0.01c_0/d$–$0.142c_0/d$. The transmission spectrum is compared with that of a homogeneous slab whose effective refractive index is $1.65n_0$ (where n_0 is the refractive index of the water background) and whose effective impedance equals ξ_0. Despite some small deviations, which may arise from higher-order diffracted waves, the transmission spectra in general agree with each other. These results verify the effective medium model we used and indicate that the impedance of the meta-surface is indeed matched to that of the water background. In comparison, we also plot in Fig. 1(b) the transmission spectrum of the meta-surface when the filling material in the slit is water. Except for a few peaks, which are attributed to the FP effect, the transmission is significantly lower than the transmission of the other two cases due to huge impedance mismatch. Here, we would like to point out that the effective medium of the structure shown in Fig. 1(a) is actually anisotropic. The rigid walls of the slits prevent the wave from propagating along the horizontal direction and the effective mass density along that direction is infinity. However, using an isotropic effective medium description would not affect the results because we only care about the *normal* incidence and the transmission and reflection coefficients of a slab of an anisotropic medium can be obtained by changing ξ_{eff} and k_{eff} in Eq. (5) into $\xi_{eff,z}$ and $k_{eff,z}$, respectively.

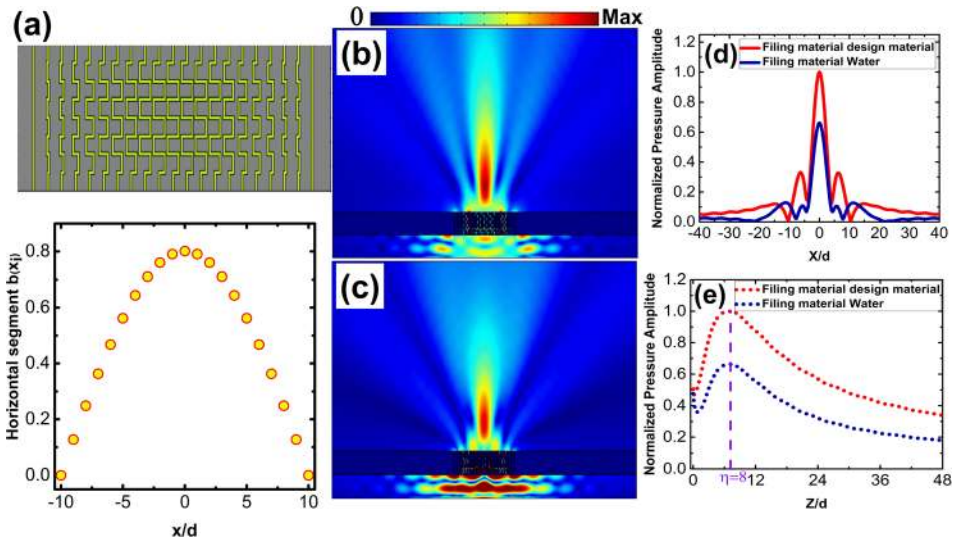

FIG. 2. (a) The upper panel is a schematic of the designed acoustic lens in water with 21 slits. The size of the horizontal segment as a function of the position of the slit is shown in the lower panel. (b) The distributions of the pressure field of a Gaussian beam at $0.141c_0/d$ frequency incident on the designed impedance-matched acoustic lens. (c) The same as (b) but the filling material inside the slits is water and the impedance does not match that of water. (d) Range and (e) cross-range distributions of the pressure fields shown in Figs. 2(b) and 2(c), respectively.

We used the coiling-up space as a building block in the acoustic lens to focus acoustic waves in water. To obtain excellent focusing without any aberration of the focal spot, we employ the following hyperbolic refractive index profile[8,24,34,35]

$$n_{eff}(x_i) = \frac{n_0}{h}\left(\sqrt{\eta^2 + x_{10}^2} - \sqrt{\eta^2 + x_i^2}\right) + n_0, \quad i = 0, 1, ..., 10, \tag{6}$$

where η is the focal length, and we let it equal $8d$. The highest value of n_{eff} occurs in the center of the lens and the lowest value occurs at the left-most and right-most slits, i.e., $n_{eff}(\pm x_{10}) = n_0$. The desired refractive index profile can be achieved by altering the total length of each slit of the acoustic lens. For simplicity but without loss of generality, we fix the number of folds of each slit to six and change the length of the horizontal segment, i.e., b, so that the total length, $h_t(x_i) = h + 6b(x_i)$, is changed accordingly. The relation between the value of b and the location of the slit is plotted in Fig. 2(a) together with a schematic of the designed lens with 21 slits, demonstrating that the maximum length of the slits is reached at the center of the lens.

To examine the performance of the acoustic lens, we conducted numerical simulations of a Gaussian beam normally incident on an acoustic lens from the bottom. We plot in Fig. 2(b) the field patterns when the frequency of the incident wave is chosen as $0.141c_0/d$. Clearly seen is a focal spot after the beam transmits though the acoustic lens. The distance from the upper surface of the acoustic lens to the focal spot is $7.76d$, which is about 0.97 times the predicted focal length. For comparison, we also plot in Fig. 2(c) the field distribution of the same wave incident on an acoustic lens with the same structure but with water as the filling material in the slit. In addition to the focusing effect, significant reflection is observed because the effective impedance of the acoustic lens is $(1/f)\xi_0$,[6] which greatly differs from the impedance of water. The normalized pressure field distribution along the horizontal and vertical directions across the center of the focal spot for both lenses is plotted, respectively, in Figs. 2(d) and 2(e). Similar patterns in the pressure field are observed for the two lenses. However, the impedance-matched lens exhibits higher intensity in the pressure field than does the other, implying that much more energy is transmitted. This focal spot with high transmission in fact appears over a frequency range of $0.107c_0/d - 0.142c_0/d$.

The foregoing analysis describes the design of a matched-impedance acoustic lens. In reality, it is difficult to find a material whose mass density and sound velocity satisfy the conditions of $\rho_s = (a/d)\,\rho_0$ and $c_s = c_0$ simultaneously to fill up the slits. However, as long as the ratio of the impedances of the material inside the slits and water is $1/f$, the impedance-matching condition is satisfied. One can adjust the length of the curled slits to meet the requirements on the effective refractive index. In the following, we describe a real sample of an acoustic lens in water. We choose isopentane (C_5H_{12}) to fill up the slits. The mass density of water and isopentane is $\rho_{\text{water}} = 1000\,\text{kg/m}^3$ and $\rho_{\text{isopentane}} = 616\,\text{kg/m}^3$. The speed of sound in water and isopentane is $c_{\text{water}} = 1490\,\text{m/s}$ and $c_{\text{isopentane}} = 980\,\text{m/s}$.[36] The width of the slit is $a = 0.4d$. The effective impedance of the acoustic lens is thus $1.5 \times 10^6\,\text{Pa s m}^{-1}$, which is very close to the impedance of water ($1.46 \times 10^6\,\text{Pa s m}^{-1}$). The speed of sound in isopentane is very different from the speed of sound in water. To satisfy the hyperbolic refractive index profile given by Eq. (6), we redesigned the coiling-up space by changing the length of the horizontal segment of each slit. In Fig. 3(a), we plot the pressure amplitude of a Gaussian

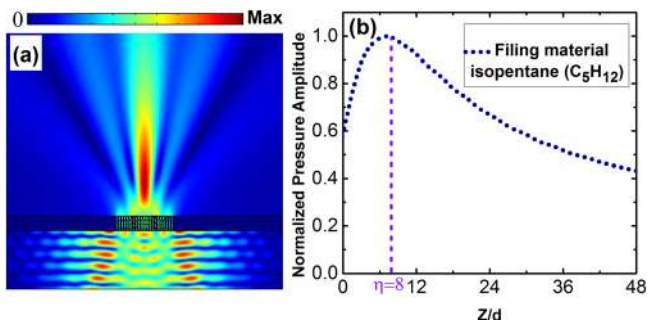

FIG. 3. (a) The pressure field distribution of a Gaussian beam at $0.154c_0/d$ frequency incident on an acoustic lens whose slits are filled with isopentane. (b) The range distribution of the pressure field shown in Fig. 3(a).

beam at $0.154c_0/d$ frequency incident on this acoustic lens. The focusing effect is clearly observed. The pressure field distribution along the incident direction across the center of the focal spot is shown in Fig. 3(b), where the maximum value of the pressure field occurs at $7.24d$, close to the predicted position of the focal point ($\eta = 8d$). It is worth mentioning that we consider the ideal fluids in our model but in reality all fluids are viscous. The viscosity of isopentane is much smaller than that of water. In a typical ultrasound experiments in water with frequency around 0.1 MHz, the thickness of viscous layer[37] is negligible compared to the width of the slit. Thus, the performance of the lens should not be seriously affected.

Properly choosing the filling material inside the slits such that the effective impedance matches the impedance of the background allows the majority of the incident wave energy to be transmitted. This selection is simple but it imposes constraints on the impedance of the filling material. Although our design for a good performance acoustic lens in water is possible, it would be very difficult to find a proper filling material that could result in an impedance-matched acoustic lens in air because the impedance of air is very low. In what follows, we introduce another design of an acoustic lens to focus acoustic waves in air. The building block of this acoustic lens is a layered medium as shown in the inset of Fig. 4(a), where argon and xenon, two noble gases, are used.[12] The material parameters of these gases are as follows: $c_{Arg} = 323\,\mathrm{m/s}$, $c_{Xen} = 169\,\mathrm{m/s}$, $\rho_{Arg} = 1.78\,\mathrm{kg/m^3}$, and $\rho_{Xen} = 5.89\,\mathrm{kg/m^3}$. We alter the thickness and sequence of the argon and xenon layers to achieve the required effective refractive index profile, i.e., Eq. (6), with the impedance matched to the impedance of the air background. This task can be accomplished by using a transfer matrix method. In each slit, the sum of the thicknesses of the two gases should be equal to the thickness of the acoustic lens, i.e., $h = h_{Arg} + h_{Xen}$, and its effective refractive index follows the relation $n_{eff}h = n_{Arg}h_{Arg} + n_{Xen}h_{Xen}$, where n_{Arg} and n_{Xen} are the refractive indices of argon and xenon, respectively. The input impedance of a medium with q layers satisfies the following recursion relation:[38]

$$\xi_{in}^{(q)} = \left[\frac{\xi_{in}^{(q-1)} - i\xi_q \tan(k_q h_q)}{\xi_q - i\xi_{in}^{(q-1)} \tan(k_q h_q)}\right]\xi_q, \tag{7}$$

where $\xi_{in}^{(q-1)}$ is the input impedance of the same layered medium without the q th layer. h_q, ξ_q, and k_q, respectively, correspond to the thickness, impedance, and wave vector of the q th layer. The reflection coefficient of such a layered medium can be determined by $R = (\xi_{in}^{(q)} - \xi_0)/(\xi_{in}^{(q)} + \xi_0)$, where ξ_0 is the impedance of the host medium. If the input impedance, $\xi_{in}^{(q)}$, is identical to ξ_0, the impedance-matching condition is satisfied, and the reflection coefficient equals zero. Eq. (7) implies that the input impedance is a function of the thickness and the arrangement of the layers, meaning that altering the sequence of the layers would result in different input impedances. Given the constraint on the respective thicknesses of argon and xenon, we have to optimize the arrangement of these two gases to achieve the best input impedance. The inset of Fig. 4(a) shows an optimized structure, where the width of the slit is $a = 0.9d$, the thickness of the plate is $h = 6d$, and the focal length is $8d$. The calculated input impedance and the reflection coefficient for an incident wave at $0.147c_0/d$ frequency in each slit are plotted in Fig. 4(a) with red and blue dots, respectively. The results indicate that the impedance is indeed matched to that of the background. A good acoustic focusing effect is achieved with the optimized design of the acoustic lens. The distributions of the amplitude of the pressure field of a Gaussian beam at $0.147c_0/d$ frequency incident normally from the bottom on the lens are shown in Fig. 4(b). A focal point is observed in the transmission domain and the reflection is weak. The location of the focal spot agrees well with the prediction. It should be mentioned that Eq. (7) is applicable because the frequency is low so that only the fundamental waveguide mode can propagate inside the slits. If the frequency becomes higher, the propagating first-order waveguide mode would first appear in the xenon layer, indicating the input impedance calculated from Eq. (7) no longer applies.

In this work, we proposed two types of impedance-matched acoustic lenses to focus acoustic waves. One is designed from the coiling-up spaces in water. From an analytic model based on coupled-mode theory, we found that a proper combination of the geometric size of the coiling-up space and its filling material would give rise to impedance that matches that of water and a desired effective refractive index. It can therefore focus the majority of the incident acoustic wave energy in water. The other type of the acoustic

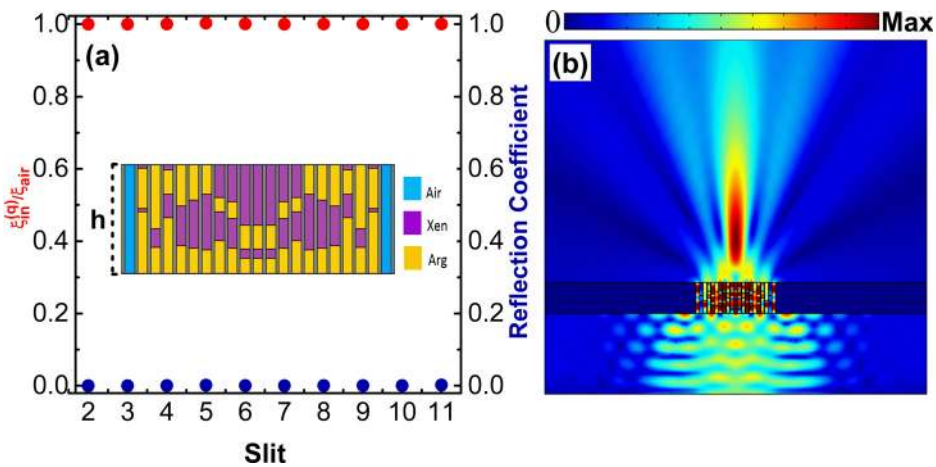

FIG. 4. (a) The input impedance and the reflection coefficient for each slit at a chosen frequency of $0.147c_0/d$. A sketch of the optimized acoustic lens in air is shown in the inset in which different colors represent different gases. (b) The distribution pressure field of a Gaussian beam at $0.147c_0/d$ frequency incident normally from the bottom on the lens.

lens was built from multi-layered media in air. We demonstrated that stacking two materials in different orders with different thicknesses would result in different effective input impedances and refractive indices. We optimized the layered structures of two gases to simulate an acoustic lens that satisfies the required impedance and refractive index conditions. High transmission and focusing of acoustic wave energy in air can be realized with such an acoustic lens. These designable lenses are experimentally feasible and may be used in applications such as collimation and redirection of beams.

The authors would like to thank Xiujuan Zhang for discussions. The work described in this paper was supported by Baseline Research Fund and Competitive Research Fund (OCRF2014CRCG62140407ORS2230) from King Abdullah University of Science and Technology.

[1]M. Fatemi and J. F. Greenleaf, Science **280**, 82 (1998).
[2]A. P. Dhawan, H. K. Huang, and D. S. Kim, *Principles and Advanced Methods in Medical Imaging and Image Analysis* (World Scientific, Stallion Press, Hackensack, NJ, 2008), pp. 129–149.
[3]J. A. Dickson and S. K. Calderwood, Nature **263**, 772 (1976).
[4]D. Torrent and J. Sanchez-Dehesa, New J. Phys. **9**, 323 (2007).
[5]F. Cervera, L. Sanchis, J. V. Sanchez-Perez, R. Martinez-Sala, C. Rubio, F. Meseguer, C. Lopez, D. Caballero, and J. Sanchez-Dehesa, Phys. Rev. Lett. **88**, 023902 (2001).
[6]P. Peng, B. Xiao, and Y. Wu, Phys. Lett. A **378**, 3389 (2014).
[7]K. Tang, C. Y. Qiu, M. Z. Ke, J. Y. Lu, Y. T. Ye, and Z. Y. Liu, Sci. Rep. **4**, 6517 (2014).
[8]Y. Li, B. Liang, X. Tao, X. F. Zhu, X. Y. Zou, and J. C. Cheng, Appl. Phys. Lett. **101**, 233508 (2012).
[9]B. Yuan, Y. Cheng, and X. Liu, Appl. Phys. Express **8**, 027301 (2015).
[10]Y. Li, B. Liang, Z. M. Gu, X. Y. Zou, and J. C. Cheng, Sci. Rep. **3**, 2546 (2013).
[11]L. Zigoneanu, B. I. Popa, and S. A. Cummer, Phys. Rev. B **84**, 024305 (2011).
[12]J. Mei and Y. Wu, New J. Phys. **16**, 123007 (2014).
[13]Y. Xie, W. Wang, H. Chen, A. Konneker, B. I. Popa, and S. A. Cummer, Nat. Commun. **5**, 5553 (2014).
[14]G. Ma, M. Yang, S. Xiao, Z. Yang, and P. Sheng, Nat. Mater. **13**, 873 (2014).
[15]K. Tang, C. Qiu, J. Lu, M. Ke, and Z. Liu, J. Appl. Phys. **117**, 024503 (2015).
[16]J. Christensen, A. I. Fernandez-Dominguez, F. De Leon-Perez, L. Martin-Moreno, and F. J. Garcia-Vidal, Nat. Phys. **3**, 851 (2007).
[17]Y. Li, B. Liang, X. Y. Zou, and J. C. Cheng, Appl. Phys. Lett. **103**, 063509 (2013).
[18]J. Zhao, B. Li, Z. N. Chen, and C. W. Qiu, Appl. Phys. Lett. **103**, 151604 (2013).
[19]J. Zhao, B. Li, Z. Chen, and C. W. Qiu, Sci. Rep. **3**, 2537 (2013).
[20]Y. Li, B. Liang, Z. M. Gu, X. Y. Zou, and J. C. Cheng, Appl. Phys. Lett. **103**, 053505 (2013).
[21]Z. X. Liang and J. Li, Phys. Rev. Lett. **108**, 114301 (2012).
[22]Y. Li, X. Jiang, B. Liang, J. C. Cheng, and L. Zhang, Phys. Rev. Appl. **4**, 024003 (2015).
[23]F. Cai, F. Liu, Z. He, and Z. Liu, Appl. Phys. Lett **91**, 203515 (2007).
[24]A. Climente, D. Torrent, and J. Sanchez-Dehesa, Appl. Phys. Lett. **97**, 104103 (2010).
[25]B. C. Gupta and Z. Ye, Phys. Rev. E **67**, 036603 (2003).
[26]A. Hakansson, J. Sanchez-Dehesa, and L. Sanchis, Phys. Rev. B **70**, 214302 (2004).
[27]C. Kuo and Z. Ye, J. Phys. D: Appl. Phys. **37**, 2155 (2004).
[28]D. Li, L. Zigoneanu, B. I. Popa, and S. A. Cummer, J. Acoust. Soc. Am. **132**, 2823 (2012).
[29]L. Sanchis, A. Hakansson, F. Cervera, and J. Sanchez-Dehesa, Phys. Rev. B **67**, 035422 (2003).
[30]Z. Liang, T. Feng, S. Lok, F. Liu, K. B. Ng, C. H. Chan, J. Wang, S. Han, S. Lee, and J. Li, Sci. Rep. **3**, 1614 (2013).
[31]Y. Xie, B. I. Popa, L. Zigoneanu, and S. A. Cummer, Phys. Rev. Lett. **110**, 175501 (2013).
[32]M. H. Lu, X. K. Liu, L. Feng, J. Li, C. P. Huang, Y. F. Chen, Y. Y. Zhu, S. N. Zhu, and N. B. Ming, Phys. Rev. Lett. **99**, 174301 (2007).
[33]B. Hou, J. Mei, M. Z. Ke, W. J. Wen, Z. Y. Liu, J. Shi, and P. Sheng, Phys. Rev. B **76**, 054303 (2007).
[34]S. C. S. Lin, T. J. Huang, J. H. Sun, and T. T. Wu, Phys. Rev. B **79**, 094302 (2009).
[35]K. Deng, Y. Q. Ding, Z. J. He, H. P. Zhao, J. Shi, and Z. Y. Liu, J. Phys. D: Appl. Phys. **42**, 185505 (2009).
[36]ONDA Corporation, Tables of Acoustic Properties of Materials, see http://www.ondacorp.com/tecref_acoustictable.shtml.
[37]J. Mei, Y. Wu, and Z. Y. Liu, Europhys. Lett. **98**, 54001 (2012).
[38]L. Brekhovskikh, *Waves in Layered Media*, 2nd ed. (Academic Press, London, 1980).